Origin of Bulk Uniaxial Anisotropy in Zinc-Blende Dilute Magnetic Semiconductors

M. Birowska,[1] C. Śliwa,[2] J. A. Majewski,[1] and T. Dietl[1,2]

[1]*Institute of Theoretical Physics, Faculty of Physics, University of Warsaw, ul. Hoża 69, PL-00-681 Warszawa, Poland*
[2]*Institute of Physics, Polish Academy of Sciences, al. Lotników 32/46, PL-02-668 Warszawa, Poland*
(Received 21 February 2012; published 7 June 2012)

It is demonstrated that the nearest-neighbor Mn pair on the GaAs (001) surface has a lower energy for the [$\bar{1}$10] direction compared to the [110] case. According to the group theory and Luttinger's method of invariants, this specific Mn distribution results in bulk uniaxial in-plane and out-of-plane anisotropies. The sign and magnitude of the corresponding anisotropy energies determined by a perturbation method and *ab initio* computations are consistent with experimental results.

One of the building blocks of condensed matter physics is the virtual crystal approximation [1,2], allowing us to extend the outcome of group theory for a given crystal symmetry to alloys with a random distribution of their constituents. However, it has been recently demonstrated, combining the progress in *ab initio* simulations and nanocharacterization methods, that the condition of the random distribution is violated in a number of alloys, leading to striking consequences. In particular, it has been found that open *d* shells of transition-metal (TM) cations diluted in nonmagnetic compounds not only provide localized spins but also, through hybridization with band states, contribute significantly to the cohesive energy, particularly when TM atoms occupy neighboring sites [3,4]. The resulting attractive force between magnetic cations leads to their aggregation, either triggered by appropriate post-growth high-temperature annealing, as found for (Ga,Mn)As [5], or occurring at the growth surface during the epitaxial process, as in the case of (Ga,Fe)N [6]. The TM aggregation invalidates the main premise of dilute magnetic semiconductor (DMS) physics, namely, that concerning the random distribution of TM spins over cation sites. One of the striking consequences is the appearance of surprising high-temperature ferromagnetism in numerous magnetically doped semiconductors and oxides, assigned now to the presence of TM aggregates [3,4].

In this paper we show that the progress in *ab initio* and nanocharacterization methods makes it possible to establish the origin of bulk crystalline in-plane uniaxial anisotropy found in magnetotransport [7–11], magnetooptical [12,13], magnetic [13–16], and ferromagnetic resonance [17] studies of (Ga,Mn)As. We show quantitatively that this puzzling anisotropy, whose presence contradicts the results of group theory for zinc-blende crystals, stems from a nonrandom distribution of Mn over cation sites, setting in at the surface during the epitaxial growth. Gaining the insight into the physical origin of the uniaxial anisotropy allows us to propose methods of its control, the important step to explore further novel functionalities in (Ga,Mn)As and related systems [18–21]. Furthermore, our model

elucidates the origin of a threefold enhancement of the shape magnetic anisotropy found in thin films of (Ga,Mn) As [11].

We consider zinc-blende (Ga,Mn)As grown by low-temperature molecular beam epitaxy (MBE) [22] along the [001] direction. Under these conditions, long-range aggregation of substitutional Mn cations is kinematically limited, as, according to three-dimensional atom probe measurements, the Mn distribution is random down to at least 1 nm [23]. Actually, the formation of Mn-rich (Mn, Ga)As nanocrystals inside (Ga,Mn)As films starts to be visible under annealing at temperatures $T_a \gtrsim 400\,°C$, considerably greater than the growth temperature $T_g \approx 200\,°C$ [5,24]. Thus, we start our studies by finding out the energetically favorable position of the nearest-neighbor (NN) Ga-substitutional Mn cation dimer on the GaAs (001) *surface*, where constituent atoms are mobile during the epitaxy. We perform *ab initio* calculations employing SIESTA code [25,26], whose localized basis is well suited for surface studies. The computations within the local-density approximation are carried out for the following supercell geometry: a pair of Mn impurities is substituted into the uppermost Ga layer of the As-terminated (001) surface of a 12 monolayers thick GaAs slab with lateral supercell dimensions of two lattice constants. In order to simulate a semi-infinite crystal, we saturate each dangling bond at the bottom Ga layer by one pseudoatom with fractional atomic number $Z = 1.25$ [27]. This guarantees, in accordance with the electron-counting model, the equal partitioning of the five As electrons over the four tetrahedral sp^3 bonds. Thus, there are in total 112 atoms in the supercell, with a 1.5 nm thick vacuum region. A $5 \times 5 \times 1$ Monkhorst-Pack grid of *k*-points is used, with the "slab dipole correction" and "simulate doping" options enabled. Since we are interested in the situation under growth conditions, we have performed a non-spin-polarized calculation with the lattice optimization.

According to the computation results, the preferred orientation of Mn dimers is along the [$\bar{1}$10] direction, with the energy gain over the NN Mn pair along [110] being as large

as 1.0 eV. Therefore, if thermal equilibrium was reached during the growth, virtually all Mn ions would form dimers oriented along the $[\bar{1}10]$ direction. Such a case can be regarded as an upper limit of the asymmetry in the actual pair distribution, as diffusion barriers may prevent attaining the free energy minimum by all Mn ions at the growth surface. Note that the Mn ions forming dimers occupy Ga-substitutional positions. Therefore, they remain stable through the further growth process, in particular, during post-growth annealing at low temperatures $T_a < T_g$ employed to diffuse out Mn in interstitial positions [28]. Among many consequences of the nonrandom Mn distribution is the appearance of a local strain, as Mn atoms in the pair are displaced of the GaAs cation positions, whereas the As atom between them is shifted along the $[00\bar{1}]$ direction by as much as 2.6% of the bond length. The resulting strain may contribute to the formation of stacking faults propagating in the (111) and $(11\bar{1})$ planes [29], observed in (Ga,Mn)As by high resolution electron transmission microscopy [30] and synchrotron x-ray diffraction [31]. Importantly, according to recent *ab initio* studies [31], the intersection lines of the stacking fault pairs may enhance further the aggregation of Mn dimers along the $[\bar{1}10]$ crystallographic directions.

In order to evaluate the effect of this specific distribution of Mn ions upon magnetic anisotropy, we assume, following the results of *ab initio* calculations, that all Mn ions form dimers oriented along the $[\bar{1}10]$ direction. Our approach consists of two steps. First, by employing the group theory and the Luttinger's method of invariants, we establish the expected form of the magnetic energy dependence on the magnetization orientation. Second, by making use of either perturbation theory or an *ab initio* method, we evaluate the magnitude of the anisotropy caused by the nonrandom Mn distribution.

In our studies, we place a nearest-neighbor (NN) Ga-substitutional Mn pair in a GaAs supercell of certain shape and dimensions. Owing to the periodic boundary conditions employed, this procedure introduces a spurious spatial correlation between the Mn dimer placed in the central supercell and its images in the neighboring supercells. In order to quantify this effect, we choose as the supercell either a cube of $N \times N \times N$ lattice constants or a parallelepiped defined by the vectors $(0, N/2, N/2)$, $(N/2, 0, N/2)$, and $(N/2, N/2, 0)$, given in units of the lattice constant (N is a natural number defining the size of the supercell). Accordingly, on imposing periodic boundary conditions, the positions of the Mn dimers form a simple cubic (sc) or face-centered cubic (fcc) superstructure, respectively, which possesses the C_{2v} point group symmetry when NN Mn pairs (dimers) are along $[\bar{1}10]$ or $[110]$ directions. Accordingly, the magnetic anisotropy energy $F(m_x, m_y, m_z)$ as a function of the magnetization direction $(m_x, m_y, m_z) = (\sin\vartheta \cos\varphi, \sin\vartheta \sin\varphi, \cos\vartheta)$ can be expanded into invariants f_i,

$$F = \sum_i K_i f_i, \tag{1}$$

where the basis invariants are defined respecting the decomposition of the space of spherical harmonics with given l into irreducible representations of the T_d group. For example, the decomposition $E \oplus T_2$ of the space of spherical harmonics with $l = 2$ defines invariants $f_1 = m_z^2 - \frac{1}{3}$ (representation E) and $f_2 = m_x m_y$ (representation T_2). These are out-of-plane and in-plane uniaxial anisotropies. For $l = 4$, the decomposition is $A_1 \oplus E \oplus T_1 \oplus T_2$, where the invariant from A_1 is the cubic anisotropy, the ones from E and T_2 are higher order uniaxial anisotropies analogous to those with $l = 2$, and there is no invariant in T_1.

Let us consider now possible NN cation configurations. Up to the translational symmetry, there are six different placements corresponding to the three planes [i.e., (100), (010), and (001)] in which a pair can be located and two possible directions in each of the planes. As the growth occurs along the [001] direction, we cannot expect the same density of dimers in the (001) plane comparing to the (100) and (010) planes. Thus, averaging of f_1 over the three planes may lead to $K_1 \neq 0$, adding to the effect of epitaxial biaxial strain. Furthermore, by symmetry, the densities of NN pairs in the two directions in the (100) and (010) planes are equal; therefore, f_2 averages to zero for each of those two planes. However, the symmetry allows a different density of NN pairs along the [110] and $[\bar{1}10]$ directions in the (001) growth surface. This results in a nonzero value of the macroscopic parameter K_2. The macroscopic value of K_2 is a product of the anisotropy energy of a single Mn pair and the difference in the densities (per supercell volume) of pairs along the [110] and $[\bar{1}10]$ directions, respectively.

More formally, the correlations in occupations between the neighboring sites form a representation of the point group T_d, which decomposes into a sum of the irreducible components, $A_1 \oplus E \oplus T_2$. The irreducible components are the total pair density (A_1), the distribution of pairs among the three planes (E), and the differences between occupations of the two directions in each of the planes (T_2). Similarly, the magnetic anisotropy free energy function decomposes into $E \oplus T_2$ (for $l = 2$) and $A_1 \oplus E \oplus T_1 \oplus T_2$ (for $l = 4$). Here, we consider a first order (linear) dependence of the magnetic anisotropy on the pair correlations. Hence, the irreducible components are in a direct correspondence: the cubic anisotropy parameter depends linearly on the total pair density (representation A_1), the out-of-plane uniaxial anisotropy parameter K_1 on the distribution of pairs among the planes (E), and the in-plane uniaxial anisotropy constant K_2 on the difference between the densities of the [110] and $[\bar{1}10]$ pairs (T_2). The remaining component, T_1, has no counterpart in the decomposition of the correlation function and therefore has to vanish. We conclude that the nonrandom distribution of Mn cations of the form introduced here leads to the functional of

the magnetic anisotropy energy [Eq. (1)] consistent with experimental results [8,11–15,17].

Previously, the anisotropy constant K_2 accounting for experimentally observed bulk uniaxial in-plane crystallographic anisotropy was described theoretically by assuming the presence of shear strain, whose magnitude ε_{xy} was treated as an adjustable parameter [15,32,33], evaluated with the $p - d$ Zener model to be of the order of $\varepsilon_{xy} \approx 0.05\%$ for the relevant GaAs deformation potential $d = -4.8$ eV [32,33]. A shear deformation appears, due to strain relaxation, in nanobars [34,35]. However, it has not been found experimentally in (Ga,Mn)As films [31]. Similarly, an additional contribution to K_1, found in studies of magnetic anisotropy as a function of biaxial strain [11], can be parameterized by $\varepsilon_{xx} \approx -0.05\%$. We will show now that new terms in the Luttinger Hamiltonian brought about by the nonrandom Mn distribution have the form of the Hamiltonian for a strain, whose components have signs and magnitudes consistent with the experimental values.

We first examine how lowering of symmetry to C_{2v} affects the three-band effective mass Hamiltonian describing the valence band in the cubic case. The spin-orbit and $p - d$ interactions can then be taken into account in the standard way, leading to the six-band Hamiltonian from which the magnetic anisotropy energy F [Eq. (1)] can be directly determined [32,33]. By employing the Luttinger's method of invariants [36], we find that the presence of spatial correlations of Mn ions is captured by the use of the virtual crystal $k \cdot p$ Hamiltonian with terms corresponding to effective shear and biaxial strains, described by two components of the strain tensor, ε_{xy} and ε_{xx}, respectively, together with the corresponding deformation potentials $d = -4.8$ eV and $b = -2.0$ eV. The effective biaxial strain ε_{xx} (with $\varepsilon_{yy} = \varepsilon_{xx}$, $\varepsilon_{zz} = -2c_{12}\varepsilon_{xx}/c_{11}$, $c_{12}/c_{11} = 0.453$) will renormalize the magnitude of strain coming from a mismatch to the substrate.

In order to evaluate the magnitude of ε_{xy} and ε_{xx}, we start from the three-band unperturbed Hamiltonian,

$$H_{3\times3}(\mathbf{k}) = E_v \mathbb{1}_{3\times3} - \frac{\hbar^2}{2m} \times \begin{bmatrix} Ak_x^2 + B(k_y^2 + k_z^2) & Ck_xk_y & Ck_xk_z \\ Ck_xk_y & Ak_y^2 + B(k_x^2 + k_z^2) & Ck_yk_z \\ Ck_xk_z & Ck_yk_z & Ak_z^2 + B(k_x^2 + k_y^2) \end{bmatrix}, \quad (2)$$

where in terms of the Luttinger parameters γ_i, $A = \gamma_1 + 4\gamma_2$, $B = \gamma_1 - 2\gamma_2$, and $C = 6\gamma_3$. The Mn potential is assumed to contain a contribution from a screened Coulomb part and a central cell correction, leading in the k space to

$$\tilde{V}(k) = \frac{e^2}{\epsilon\epsilon_0}\frac{1}{k^2 + r_s^{-2}} + \pi^{(3/2)}V_0 r_0^3 e^{-k^2 r_0^2/4}, \quad (3)$$

where the static dielectric constant $\epsilon = 12.9$, the screening radius is $r_s = 0.5$ nm [37], and the Gaussian central cell correction parameters are $r_0 = 0.28$ nm, $V_0 = 3.0$ eV [38].

Within the second order perturbation theory for a Mn pair we obtain at $\mathbf{k} = 0$,

$$\Delta H_{3\times3}^{(2)} = g_\mathbf{d} \int \frac{d^3\mathbf{k}}{(2\pi)^3}\left(2\cos\frac{\mathbf{k}\cdot\mathbf{d}}{2}\right)^2 |\tilde{V}(k)|^2$$
$$\times [E_v \mathbb{1}_{3\times3} - H_{3\times3}(\mathbf{k})]^{-1}, \quad (4)$$

where $\mathbf{d}$ is the vector between the two Mn ions forming the pair and $g_\mathbf{d}$ is the density of such pairs. In the case of a supercell, the integral should be replaced with a sum over the reciprocal lattice $\int\frac{d^3\mathbf{k}}{(2\pi)^3} \to \frac{1}{V_{sc}}\sum_{\mathbf{k}\neq0}$, where $\mathbf{k} = 0$ is omitted from the sum and V_{sc} is the volume of the supercell. The above formula assumes additivity of the Mn potential and neglects distortion of the lattice in the presence of the Mn pair. A similar formula without the squared cosine factor can be used to determine the anisotropy of a

single Mn acceptor in a noncubic supercell [39], as a single Mn acceptor residing in a supercell exhibits a significant magnetic anisotropy in accord with the symmetry of the supercell. In agreement with the symmetry considerations, $\Delta H_{3\times3}^{(2)}$ given by Eq. (4) can be parameterized by the effective strain tensor components ε_{xy} and ε_{xx} according to

$$\Delta H_{3\times3}^{(2)} = \begin{bmatrix} P - Q & R & 0 \\ R & P - Q & 0 \\ 0 & 0 & P + 2Q \end{bmatrix}, \quad (5)$$

where in terms of the deformation potentials b and d,

$$\varepsilon_{xy} = \frac{R}{\sqrt{3}d}, \qquad \varepsilon_{xx} = -\frac{c_{11}}{c_{11} + 2c_{12}}\frac{Q}{b}. \quad (6)$$

The obtained results are presented in Fig. 1 for the NN Mn pair residing along the preferred direction $[\bar{1}10]$. In particular, in the case of no supercell, that is when positions of the $[\bar{1}10]$ dimers can be regarded as uncorrelated, we obtain $\varepsilon_{xy}/g_\mathbf{d} = 0.019$ nm^3, $\varepsilon_{xx}/g_\mathbf{d} = -0.0015$ nm^3. For the Mn concentration $x = 6.25\%$, this leads to $\varepsilon_{xy} = 1.33\%$, $\varepsilon_{xx} = -0.10\%$. However, when the positions of the $[\bar{1}10]$ dimers are correlated, $\varepsilon_{xy} = 0.70\%$, $\varepsilon_{xx} = -0.26\%$ in the case of a 32 cations sc supercell and $\varepsilon_{xy} = 0.77\%$, $\varepsilon_{xx} = -0.16\%$ in the case of a 27 cations fcc supercell, corresponding to (Ga,Mn)As with 6.25% and 7.41% of Mn arranged into a regular superlattice of $[\bar{1}10]$
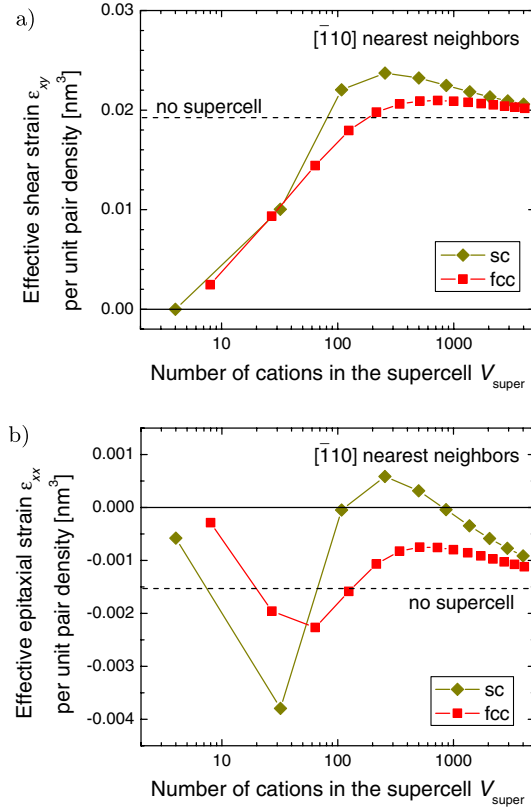
FIG. 1 (color online). Effective shear ε_{xy} (a) and epitaxial biaxial ε_{xx} (b) strains, normalized to unit pair density, for nearest-cation neighbor $[\bar{1}10]$ pairs of Mn ions in supercells arranged in simple cubic and face-centered superlattices, as calculated by using Eq. (4).

Mn dimers. Interestingly, both ε_{xy} and ε_{xx} show a non-monotonic dependence on the number of cations in the supercell. This behavior confirms that an additional periodicity imposed by the supercell method may affect the computed values quantitatively or even qualitatively, for instance, leading to the sign reversal visible in Fig. 1(b).

Comparing to experimental findings, we see that the computed values of ε_{xy} and ε_{xx} have the correct sign. At the same time, their absolute values are significantly greater than the one determined experimentally, $\varepsilon_{xy} \approx 0.05\%$ and $\varepsilon_{xx} \approx -0.05\%$. This could be expected, as in real samples only a fraction of the Mn content forms NN pairs as well as some Mn pairs choose the less preferred direction during the growth process.

It is instructive to compare the above findings to *ab initio* result. For these calculations particularly suitable is the QUANTUM ESPRESSO code developed in the plane wave basis [40]. Within local spin density approximation and for supercells with 32 cations (sc) and 27 cations (fcc), using a $4 \times 4 \times 4$ grid of k points, we obtain from magnitudes of the valence band splitting at the Γ point of the Brillouin zone, $\varepsilon_{xy} = 1.37\%$ (1.50%), $\varepsilon_{xx} = -0.49\%$ (-0.47%) and $\varepsilon_{xy} = 1.70\%$ (1.79%), $\varepsilon_{xx} = -0.75\%$

(-1.01%) without (with) lattice optimization, respectively. We note that while neither second order perturbation theory nor current *ab initio* methods can serve to describe transport phenomena in the presence of quantum localization, they appear sufficiently accurate for evaluating thermodynamic properties, including magnetic anisotropy.

In summary, we argue that puzzling bulk in-plane crystalline magnetic anisotropy in (Ga,Mn)As films grown along [001] direction is brought about by the preferred formation of Mn dimers along the $[\bar{1}10]$ at the growth surface, as implied by the *ab initio* results. The group theory and the Luttinger's method of invariants as well as the perturbation and *ab initio* computation results show that the effect of the predicted Mn distribution can be parameterized by effective shear and biaxial strains. Their signs agree with the experimental determination while the computed absolute values are much larger than the experimental magnitudes, indicating that the surplus of Mn dimers residing in the preferred positions is only partial after the growth process. This suggests that it might be possible to control the strength of uniaxial anisotropy by changing the epitaxy conditions, particularly the growth rate and/or temperature. Furthermore, when reducing the film thickness, interfacial and surface anisotropies, which feature an in-plane uniaxial anisotropy component even for a random distribution of magnetic ions [41,42], may gradually come into play. In general terms, our results show how a specific microscopic distribution of alloy constituents may affect the symmetry properties and magnitudes of macroscopic response functions.

[1] L. Nordheim, Ann. Phys. (Leipzig) **401**, 607 (1931).
[2] L. Nordheim, Ann. Phys. (Leipzig) **401**, 641 (1931).
[3] K. Sato, L. Bergqvist, J. Kudrnovský, P. H. Dederichs, O. Eriksson, I. Turek, B. Sanyal, G. Bouzerar, H. Katayama-Yoshida, V. A. Dinh, T. Fukushima, H. Kizaki, and R. Zeller, Rev. Mod. Phys. **82**, 1633 (2010).
[4] A. Bonanni and T. Dietl, Chem. Soc. Rev. **39**, 528 (2010).
[5] J. De Boeck, R. Oesterholt, A. Van Esch, H. Bender, C. Bruynseraede, C. Van Hoof, and G. Borghs, Appl. Phys. Lett. **68**, 2744 (1996).
[6] A. Navarro-Quezada, N. Gonzalez Szwacki, W. Stefanowicz, T. Li, A. Grois, T. Devillers, M. Rovezzi, R. Jakieła, B. Faina, J. A. Majewski, M. Sawicki, T. Dietl, and A. Bonanni, Phys. Rev. B **84**, 155321 (2011).
[7] S. Katsumoto, A. Oiwa, Y. Iye, H. Ohno, F. Matsukura, A. Shen, and Y. Sugawara, Phys. Status Solidi B **205**, 115 (1998).

PHYSICAL REVIEW LETTERS

[8] H. X. Tang, R. K. Kawakami, D. D. Awschalom, and M. L. Roukes, Phys. Rev. Lett. **90,** 107201 (2003).

[9] C. Gould, K. Pappert, G. Schmidt, and L. W. Molenkamp, Adv. Mater. **19,** 323 (2007).

[10] C. Gould, S. Mark, K. Pappert, R. G. Dengel, J. Wenisch, R. P. Campion, A. W. Rushforth, D. Chiba, Z. Li, X. Liu, W. Van Roy, H. Ohno, J. K. Furdyna, B. Gallagher, K. Brunner, G. Schmidt, and L. W. Molenkamp, New J. Phys. **10,** 055007 (2008).

[11] M. Glunk, J. Daeubler, L. Dreher, S. Schwaiger, W. Schoch, R. Sauer, W. Limmer, A. Brandlmaier, S. T. B. Goennenwein, C. Bihler, and M. S. Brandt, Phys. Rev. B **79,** 195206 (2009).

[12] D. Hrabovsky, E. Vanelle, A. R. Fert, D. S. Yee, J. P. Redoules, J. Sadowski, J. Kanski, and L. Ilver, Appl. Phys. Lett. **81,** 2806 (2002).

[13] U. Welp, V. K. Vlasko-Vlasov, X. Liu, J. K. Furdyna, and T. Wojtowicz, Phys. Rev. Lett. **90,** 167206 (2003).

[14] U. Welp, V. K. Vlasko-Vlasov, A. Menzel, H. D. You, X. Liu, J. K. Furdyna, and T. Wojtowicz, Appl. Phys. Lett. **85,** 260 (2004).

[15] M. Sawicki, K.-Y. Wang, K. W. Edmonds, R. P. Campion, C. R. Staddon, N. R. S. Farley, C. T. Foxon, E. Papis, E. Kamińska, A. Piotrowska, T. Dietl, and B. L. Gallagher, Phys. Rev. B **71,** 121302 (2005).

[16] Y. S. Kim, Z. G. Khim, J. Yoon, Y. Jo, M.-H. Jung, H. K. Choi, Y. D. Park, S. K. Jerng, and S. H. Chun, J. Korean Phys. Soc. **50,** 839 (2007).

[17] X. Liu, Y. Sasaki, and J. K. Furdyna, Phys. Rev. B **67,** 205204 (2003).

[18] J. Wunderlich, T. Jungwirth, B. Kaestner, A. C. Irvine, A. B. Shick, N. Stone, K.-Y. Wang, U. Rana, A. D. Giddings, C. T. Foxon, R. P. Campion, D. A. Williams, and B. L. Gallagher, Phys. Rev. Lett. **97,** 077201 (2006).

[19] D. Chiba, M. Sawicki, Y. Nishitani, Y. Nakatani, F. Matsukura, and H. Ohno, Nature (London) **455,** 515 (2008).

[20] A. Chernyshov, M. Overby, X. Liu, J. K. Furdyna, Y. Lyanda-Geller, and L. P. Rokhinson, Nature Phys. **5,** 656 (2009).

[21] M. Endo, F. Matsukura, and H. Ohno, Appl. Phys. Lett. **97,** 222501 (2010).

[22] H. Ohno, Science **281,** 951 (1998).

[23] M. Kodzuka, T. Ohkubo, K. Hono, F. Matsukura, and H. Ohno, Ultramicroscopy **109,** 644 (2009).

[24] J. Sadowski, J. Z. Domagala, R. Mathieu, A. Kovács, T. Kasama, R. E. Dunin-Borkowski, and T. Dietl, Phys. Rev. B **84,** 245306 (2011).

[25] P. Ordejón, E. Artacho, and J. M. Soler, Phys. Rev. B **53,** R10 441 (1996).

[26] J. M. Soler, E. Artacho, J. D. Gale, A. Garcá, J. Junquera, P. Ordejón, and D. Sánchez-Portal, J. Phys. Condens. Matter **14,** 2745 (2002).

[27] Pseudoatoms are the objects representing atoms in which the interaction between a valence electron and the nucleus screened by core electrons is described by a pseudopotential. Pseudopotentials with a fractional charge Z can be generated using a tool distributed with the SIESTA code.

[28] K. M. Yu, W. Walukiewicz, T. Wojtowicz, I. Kuryliszyn, X. Liu, Y. Sasaki, and J. K. Furdyna, Phys. Rev. B **65,** 201303 (2002).

[29] Y. Ohno, N. Adachi, and S. Takeda, Appl. Phys. Lett. **83,** 54 (2003).

[30] X. Kong, A. Trampert, X. X. Guo, L. Daweritz, and K. H. Ploog, J. Appl. Phys. **97,** 036105 (2005).

[31] M. Kopecký, J. Kub, F. Máca, J. Mašek, O. Pacherová, A. W. Rushforth, B. L. Gallagher, R. P. Campion, V. Novák, and T. Jungwirth, Phys. Rev. B **83,** 235324 (2011).

[32] J. Zemen, J. Kučera, K. Olejník, and T. Jungwirth, Phys. Rev. B **80,** 155203 (2009).

[33] W. Stefanowicz, C. Śliwa, P. Aleshkevych, T. Dietl, M. Döppe, U. Wurstbauer, W. Wegscheider, D. Weiss, and M. Sawicki, Phys. Rev. B **81,** 155203 (2010).

[34] S. Humpfner, K. Pappert, J. Wenisch, K. Brunner, C. Gould, G. Schmidt, L. W. Molenkamp, M. Sawicki, and T. Dietl, Appl. Phys. Lett. **90,** 102102 (2007).

[35] D. Fang, H. Kurebayashi, J. Wunderlich, K. Výborný, L. P. Zârbo, R. P. Campion, A. Casiraghi, B. L. Gallagher, T. Jungwirth, and A. J. Ferguson, Nature Nanotech. **6,** 413 (2011).

[36] G. L. Bir and G. E. Pikus, *Symmetry and Strain-Induced Effects in Semiconductors* (John Wiley & Sons, New York, 1974).

[37] M. P. López-Sancho and L. Brey, Phys. Rev. B **68,** 113201 (2003).

[38] A. K. Bhattacharjee and C. Benoit à la Guillaume, Solid State Commun. **113,** 17 (1999).

[39] T. O. Strandberg, C. M. Canali, and A. H. MacDonald, Phys. Rev. B **80,** 024425 (2009).

[40] P. Giannozzi, S. Baroni, N. Bonini, M. Calandra, R. Car, C. Cavazzoni, D. Ceresoli, G. L. Chiarotti, M. Cococcioni, I. Dabo, A. Dal Corso, S. de Gironcoli, S. Fabris, G. Fratesi, R. Gebauer, U. Gerstmann, C. Gougoussis, A. Kokalj, M. Lazzeri, L. Martin-Samos, N. Marzari, F. Mauri, R. Mazzarello, S. Paolini, A. Pasquarello, L. Paulatto, C. Sbraccia, S. Scandolo, G. Sclauzero, A. P. Seitsonen, A. Smogunov, P. Umari, and R. M. Wentzcovitch, J. Phys. Condens. Matter **21,** 395502 (2009).

[41] M. Sawicki, F. Matsukura, A. Idziaszek, T. Dietl, G. M. Schott, C. Ruester, C. Gould, G. Karczewski, G. Schmidt, and L. W. Molenkamp, Phys. Rev. B **70,** 245325 (2004).

[42] S. Mankovsky, S. Polesya, S. Bornemann, J. Minár, F. Hoffmann, C. H. Back, and H. Ebert, Phys. Rev. B **84,** 201201 (2011).